

1 **MODELLING SALINITY EFFECTS ON AEROBIC GRANULAR SLUDGE**  
2 **TREATING FISH-CANNING WASTEWATER**

3 **P. Carrera<sup>a,b\*</sup>, L. Strubbe<sup>b</sup>, A. Val del Río<sup>a</sup>, A. Mosquera-Corral<sup>a</sup>, E.I.P. Volcke<sup>b</sup>**

4 <sup>a</sup> CRETUS Institute. Department of Chemical Engineering, Universidade de Santiago de  
5 Compostela. E-15782, Santiago de Compostela, Spain

6 <sup>b</sup> BioCo Research Group, Department of Green Chemistry and Technology, Ghent University,  
7 Coupure Links 653, 9000 Gent, Belgium

8 \*Corresponding author: Paula Carrera (Paula.CarreraFernandez@UGent.be)

9

10 Accepted manuscript of the article:

11 P. Carrera, L. Strubbe, A. Val del Río, A. Mosquera-Corral, E.I.P. Volcke (2023). Modelling  
12 salinity effects on aerobic granular sludge treating fish-canning wastewater. Environ. Sci.:  
13 Water Res.Technol., 2023, 9, 747. DOI: 10.1039/d2ew00874b.

14

15 **KEYWORDS**

16 Aerobic granular sludge; industrial wastewater; salinity; biokinetic model

17 **ABSTRACT**

18 The effect of salinity on aerobic granular sludge treating fish-canning wastewater was  
19 evaluated through a one-dimensional biofilm model. Salt inhibition of heterotrophic and  
20 nitrifying bacteria was described by a non-competitive inhibition term, for which the value of  
21 the inhibition coefficient was estimated based on data from literature. The model was calibrated  
22 and validated with experimental lab-scale data regarding COD and nitrogen removal from

23 industrial wastewater. Two dynamic operating periods with salinities of 13 and 5 g NaCl/L  
24 were used for calibration and validation, respectively. The prevailing feast-famine regime  
25 necessitated simultaneous growth and storage processes to accurately describe COD removal.  
26 The presence of salt caused nitrite accumulation, as well as unusually low estimated maximum  
27 growth rates of nitrifying bacteria. The addition of a salinity inhibition term to the model could  
28 accurately describe the COD and nitrogen species experimentally measured along the cycles  
29 with different salinities.

## 30 **1. INTRODUCTION**

31 The Aerobic Granular Sludge (AGS) technology is nowadays regarded as an established way  
32 to treat both municipal and industrial wastewater, resulting in significant space and energy  
33 savings compared with traditional activated sludge processes [1]. In order to profit from these  
34 benefits, there has been an increasing interest to also treat saline wastewater with AGS. This  
35 includes Wastewater Treatment Plants (WWTP) from urban areas located in coastal areas,  
36 which have infiltrations of saline groundwater [2,3], as well as from different industrial sectors,  
37 such as the petrochemical industry [4] or seafood processing [5,6].

38 High salt concentrations affect the reactor performance through their effect on both the physical  
39 properties of the granules and biological activity. Overall, saline wastewater, with moderate  
40 salt concentrations (5 – 15 g NaCl/L), can be beneficial for the formation of dense and smooth  
41 aerobic aggregates with good settling properties [7]. The presence of salt provokes an increase  
42 of the bulk liquid density and leads to the washout of light and poor settling aggregates [8]. As  
43 a consequence, there is a reduction of the biomass concentration in the system, where only the  
44 dense aggregates with good settleability are present. In addition, the growth of granules with a  
45 regular and smooth surface is promoted and the production of extracellular polymeric  
46 substances is increased [9,10].

47 However, high salinity has been reported to have a detrimental effect on biological activity.  
48 Different inhibition thresholds have been observed depending on (1) the tolerance of each type  
49 of bacteria and (2) the adaptation of the biomass to high salt concentrations. The inhibitory  
50 effect of salinity has been studied mostly on nitrifying bacteria, whereas less research works  
51 paid attention to salt inhibition of heterotrophic bacteria. In general, salt concentrations lower  
52 than 10 g NaCl/L do not significantly affect the biological activity. However, when the salt  
53 content is above 10 g NaCl/L, the biological activity is usually reduced [11]. For example,  
54 batch tests performed by Bassin et al. [8] showed a complete inhibition of the ammonium  
55 uptake rate at a salt concentration of 20 g NaCl/L without previous acclimatization of AGS to  
56 salinity. Li et al. [10] observed an almost complete inhibition of NOB with salinities higher  
57 than 6 g NaCl/L. Moreover, Wang et al. [11] reported an important AOB activity reduction  
58 (20% of the initial value) with salt concentrations above 15 g NaCl/L. If the biomass is adapted  
59 to salinity, both AOB and NOB are usually able to withstand higher salt concentrations. For  
60 example, Bassin et al. [8] and Pronk et al. [12] reported complete inhibition of salinity-adapted  
61 NOB with a salt concentration of 33 g NaCl/L and 20 g Cl<sup>-</sup>/L, respectively. Most of the studies  
62 agree that NOB are more sensitive than AOB to high salt concentrations [8,12,13]. However,  
63 a few have reported the opposite behaviour [11,14].

64 Modelling is a useful tool to gain understanding in and to optimize the biological processes  
65 involved in wastewater treatment. The Activated Sludge Models (ASM) have been used to  
66 simulate the bioconversion processes that occur in AGS reactors. Depending on the specific  
67 reactor configuration, different biological processes take place, and thus, different ASM  
68 models are used [15]. Aerobic granular sludge reactors removing organic carbon, nitrogen and  
69 phosphorus are best described with ASM2-ASM2d models, which consider Phosphate  
70 Accumulating Organisms (PAO) activity [16]. On the other hand, in AGS reactors with a short  
71 feeding phase, only organic carbon and nitrogen conversion processes take place. In this case,

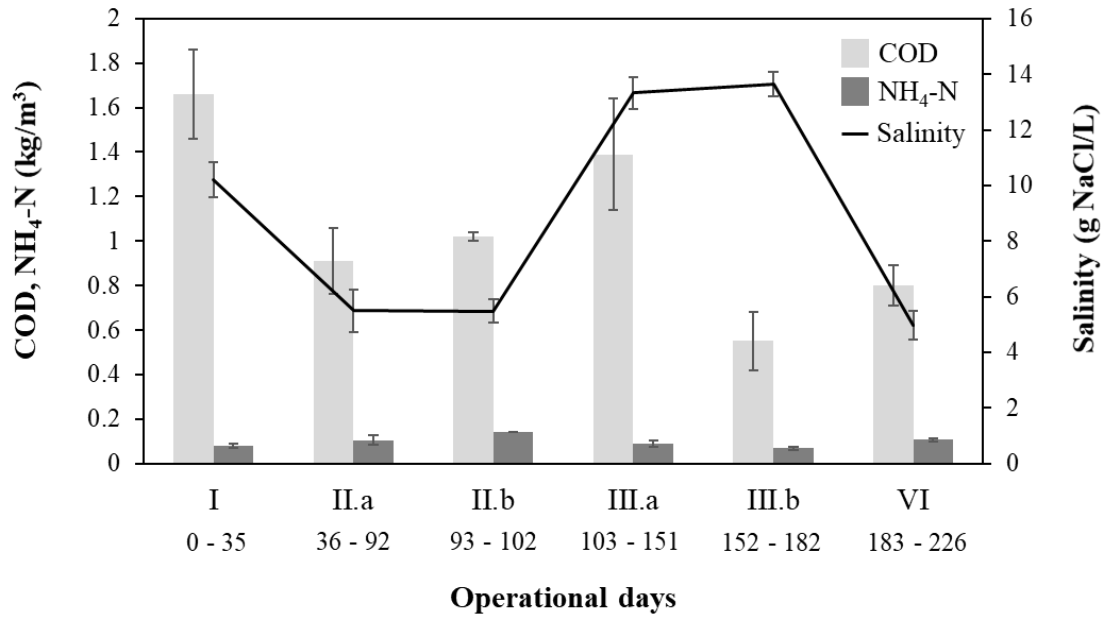
72 ASM1 and ASM3 [16] are sufficient to model the reactor performance. Although ASM models  
73 have been successfully applied to simulate many case studies [15], none of them has addressed  
74 the treatment of saline wastewater and explicitly considered the salinity effect on the biological  
75 activity of AGS.

76 In this study, a model was set up to describe the operation of an AGS treating industrial saline  
77 wastewater. Several research objectives were defined for this purpose. First, the best approach  
78 to describe the biological conversions was evaluated by comparing alternative models against  
79 each other (ASM1 versus ASM3). Second, the need to consider an inhibition term to include  
80 the effect of salinity was investigated. Third, the value for the inhibition constant was estimated  
81 based on literature data. Finally, the model was calibrated and validated under dynamic (cyclic)  
82 reactor operation, treating influent with different salt concentrations.

## 83 **2. MATERIALS AND METHODS**

### 84 **2.1. Experimental data**

85 The operating conditions of an AGS reactor fed with saline wastewater from a fish-canning  
86 industry, described by Carrera et al. [7], were taken as a reference scenario. The reactor had a  
87 working volume of 1.7 L and a volume exchange ratio of 50%. The feeding strategy consisted  
88 of pulse feeding followed by aeration (no anaerobic feeding). The length of the operational  
89 cycles was 4 h, distributed as follows: 5 min of feeding, 227 min of aeration, 1 min of settling  
90 and 7 min of effluent withdrawal. During the aeration phase, the dissolved oxygen  
91 concentration reached saturation values of 8.6 mg O<sub>2</sub>/L. The reactor operation was divided into  
92 different phases, corresponding to different batches of wastewater (Figure 1). The changes in  
93 wastewater composition (salt, COD and nitrogen concentration) were associated to the seasonal  
94 variations of the processed fish products in the factory - no adjustments were made by the  
95 authors.



96

97 Figure 1: Influent characterization of the AGS reactor in terms of soluble COD, ammonia and salt  
 98 concentration. Provided data are average values plus standard deviation corresponding to the analytical  
 99 measurements performed in each phase.

100 The experimental data selected for model calibration and validation corresponded to two  
 101 operational phases where the reactor was operating in steady-state conditions (fully-granular  
 102 system, stable nitrifying and heterotrophic activity). In particular, the dataset corresponding to  
 103 phase III.b was selected for calibration, since the reactor was operated with the highest salt  
 104 concentration (13 g NaCl/L). Relatively constant biomass concentration and effluent  
 105 composition were observed during the entire stage. Thus, it was considered to be at steady-  
 106 state conditions [7]. For validation, the experimental data from phase IV was used, with an  
 107 influent salt concentration of 5 g NaCl/L. In this stage, biomass washout occurred due to the  
 108 decrease of salinity, but the effluent concentrations were relatively constant. Detailed  
 109 information related to the operational conditions of the reactor used as input of the model is  
 110 presented in Table S.1. More detailed information about the reactor operation can be found in  
 111 Carrera et al. [7].

### 112 3. AEROBIC GRANULAR SLUDGE REACTOR MODEL

#### 113 3.1. Bioconversion models

114 Both ASM1 and ASM3 [17] were applied to describe the organic carbon and nitrogen  
115 conversions in the AGS reactor. Both models include the growth and decay processes of  
116 heterotrophs and autotrophs, and the hydrolysis of organic matter and nitrogen compounds.  
117 However, ASM1 considers direct biomass growth on substrate, whereas ASM3 assumes that  
118 substrates are first stored and biomass growth subsequently takes place on storage polymers.

119 Two modifications were made for an accurate description of the biological processes in the  
120 AGS reactor under study. The first modification of the model was the description of  
121 nitrification as a two-step process, involving the oxidation of ammonia to nitrite by AOB, and  
122 the subsequent oxidation of nitrite to nitrate by NOB, as done in previous studies [18,19].  
123 Nitrite was also included as an intermediate compound in the denitrification processes. This  
124 modification is especially important when treating saline wastewater, since in many cases NOB  
125 can be inhibited due to the presence of salt. ASM3 with the abovementioned modifications has  
126 been successfully applied in a few studies modelling AGS reactors [20–24]. This modification  
127 was applied to both ASM1 and ASM3.

128 The second modification was the introduction of simultaneous growth and storage by  
129 heterotrophic bacteria, as proposed by Krishna and Van Loosdrecht [25]. Indeed, in systems  
130 with pulse feeding followed by aeration (aerobic feast-famine), both storage and growth take  
131 place at the same time under feast conditions. So, in order to provide an accurate description  
132 of the process, direct biomass growth on soluble COD was included in the model, in addition  
133 to growth based on stored polymers. This modification was applied only to ASM3, since ASM1  
134 does not include storage processes.

135 The developed model included 7 soluble and 5 particulate compounds (Table S.2). The soluble  
136 compounds were dissolved oxygen ( $S_O$ ), soluble easily biodegradable COD ( $S_S$ ), soluble inert  
137 COD ( $S_I$ ), organic nitrogen ( $S_{ND}$ ), ammonium ( $S_{NH}$ ), nitrite ( $S_{NO_2}$ ) and nitrate ( $S_{NO_3}$ ). The  
138 particulate compounds comprised: particulate slowly biodegradable COD ( $X_S$ ), particulate  
139 inert COD ( $X_I$ ), heterotrophic bacteria (HB,  $X_H$ ), storage compounds ( $X_{STO}$ ), AOB ( $X_A$ ), and  
140 NOB ( $X_N$ ). Alkalinity was not included in the model because it was not a limiting process  
141 parameter. In addition, pH and temperature were considered constant, due to the low  
142 fluctuations during each operational phase of the SBR operation (7.2 – 7.5 and 22.6 – 23.8°C  
143 for pH and temperature, respectively). The soluble COD concentration ( $S_{COD}$ ), calculated as  
144 the sum of soluble inert COD ( $S_I$ ) and soluble easily biodegradable COD ( $S_S$ ), was included in  
145 the model as an additional output variable, for comparison with the experimentally-measured  
146 soluble COD concentration. The stoichiometric matrix of soluble and particulate compounds  
147 is presented in Table S.3. All bioconversion reactions included in the model are listed in Table  
148 S.4.

### 149 **3.2. SBR operation**

150 To describe the discontinuous operation of the SBR in Aquasim, the total reactor volume was  
151 divided into a biofilm reactor compartment and a mixed reactor compartment. They were  
152 coupled with a diffusive link (exchange coefficient 1000 m<sup>3</sup>/h) to let the liquid phase behave  
153 as one perfectly mixed water volume and ensure the same bulk liquid concentration in both  
154 compartments [26]. The volume of the biofilm compartment was fixed at 0.25 L. It was defined  
155 as a confined reactor type with rigid biofilm matrix. The completely mixed reactor contained  
156 the remaining liquid, and had a variable volume. The maximum value was 1.7 L during the  
157 aeration phase.

158 The transport processes inside the granules, which are influenced by diffusion coefficients,  
 159 density and porosity were described through Aquasim. Mass transfer resistance from the bulk  
 160 liquid to the granule surface was neglected. To model the intragranular transport, a compound-  
 161 specific estimation of the effective diffusion coefficient inside a biofilm matrix was used [27].  
 162 The granule depth was divided into 20 grid points.

### 163 3.3. Description of salinity effects

164 The effect of salinity on biological activity was considered as a non-competitive inhibition.  
 165 Different terms have been proposed in literature to describe this type of inhibition in bacteria  
 166 (Table S.6). In this study, the inhibition term was added to the growth processes of all the types  
 167 of bacteria (AOB, NOB and heterotrophs).

$$\frac{K_{Inh,50}}{K_{Inh,50} + S_{Inh}} \quad (\text{Eq.1})$$

168 The value of the half-saturation constants was estimated based on activity tests of different  
 169 research works, that report a reduction of the biological activity with the increase of salinity.  
 170 Different parameter values were obtained for biomass non-adapted or adapted to salinity (Table  
 171 1). A detailed description of the estimation of this parameter is provided in the results and  
 172 discussion section.

173 Table 1: Estimated values for the saturation constant ( $K_{Inh,50}$ ) of the inhibition term ( $\frac{K_{Inh,50}}{K_{Inh,50} + S_{Inh}}$ ).

<b>Bacteria</b>	<b><math>K_{Inh,50}</math> (g/L)</b>	<b>Salinity adaptation</b>
AOB	10.7 ± 3.2	No
	24.8 ± 9.5	Yes
NOB	13.5 ± 0.0	No
	21.7 ± 5.5	Yes
HB	23.0 ± 0.0	No
	44.3 ± 10.4	Yes

174



### 175 **3.4. Simulation set-up**

176 Simulations were done for constant influent composition, corresponding to the measured  
177 average values of each operational phase (Table S.1). The simulations were run with the  
178 reference operational conditions (Table S.1) for 200 days to ensure a steady-state operation and  
179 microbial population distribution. The operation was considered at stationary state conditions  
180 when the effluent concentrations profiles of all compounds were the same (within less than 5%  
181 difference with respect to the final value) in at least two consecutive cycles and also the spatial  
182 profiles of all biomass types inside the granule remained unchanged. The model was  
183 implemented in the Aquasim simulation software [28].

184 To calibrate the model, the simulation was first run with default values of the kinetic  
185 parameters, provided by ASM1 and ASM3 [16]. The COD, NH<sub>4</sub>-N, NO<sub>2</sub>-N and NO<sub>3</sub>-N profiles  
186 obtained with the model were compared with experimental data from a representative cycle per  
187 operating phase, corresponding to the conditions used as input of the model. Model calibration  
188 was performed sequentially, firstly focused on COD removal, and afterwards nitrogen removal,  
189 as suggested by Rittman et al. [29]. To do that, the half-saturation coefficients were maintained,  
190 whereas the maximum growth rates were modified.

191

## 192 **4. RESULTS AND DISCUSSION**

### 193 **4.1. Evaluation of ASM1**

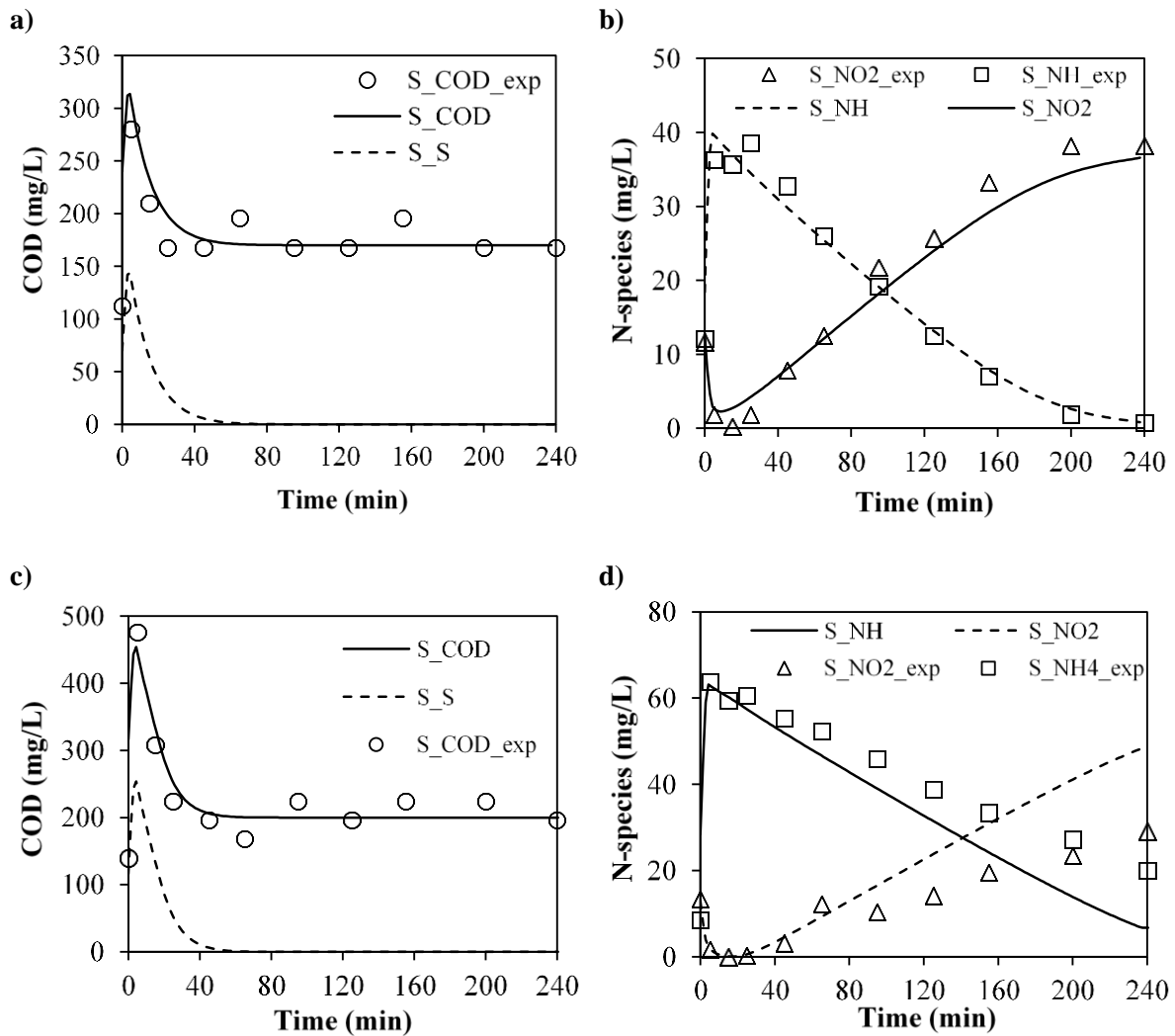
194 The SBR operation was first simulated based on ASM1, to evaluate what could be achieved  
195 with a relatively simple model (compared to ASM3). To fit the experimental data (from phase  
196 III.b) in terms of COD conversion rate, the maximum growth rate of heterotrophic bacteria was  
197 estimated at the maximum of the tested range, namely  $\mu_{\max,H} = 20 \text{ d}^{-1}$  (Figure S.2). This value  
198 seemed unreasonably high compared to ASM1 and ASM3 models describing the operation of

199 AGS reactors, which were in a range of 2 [16] – 13 d<sup>-1</sup> [30]. Therefore, ASM1, in which COD  
200 removal is only associated to biomass growth, did not provide an accurate description of the  
201 biological processes occurring inside the reactor for organics removal. Since it was not possible  
202 to reproduce the same COD conversion rates of the experimental data, ASM1 was discarded  
203 and subsequent ASM3 implementation was tested.

#### 204 **4.2. Calibration of ASM3**

205 Using ASM3, it was possible to reproduce the COD and N conversion rates observed  
206 experimentally. This indicates the need to consider the storage processes, in addition to biomass  
207 growth, to explain the COD conversion rates. For this reason, ASM3 (and not ASM1) is the  
208 most suitable model to simulate the performance of an AGS reactor with short feeding phase.  
209 At this point, salinity inhibition was not yet explicitly considered in the model, in order to  
210 describe the observed reactor performance with the simplest model possible. More specifically,  
211 it was evaluated whether the estimated kinetic parameters were in a realistic range.

212 The results of the ASM3 calibration showed the consumption of all biodegradable COD in the  
213 first minutes of the cycle, during the feast phase (Figure 2.a). The COD present at the end of  
214 the cycle was attributed to the inert fraction (fractionation tests showed a S<sub>I</sub> concentration of  
215 170 g COD·m<sup>-3</sup>, see Table S.1). Ammonia was completely oxidized to nitrite, whereas further  
216 oxidation to nitrate did not take place (nitrification activity not detected) (Figure 2.b). This  
217 agreed with the experimental findings, where the presence of nitrate and NOB were measured,  
218 but not detected due to salt inhibition (more details in Carrera et al. [7]). In addition, during the  
219 first minutes of the cycle, denitrification of nitrite from the previous cycle took place.

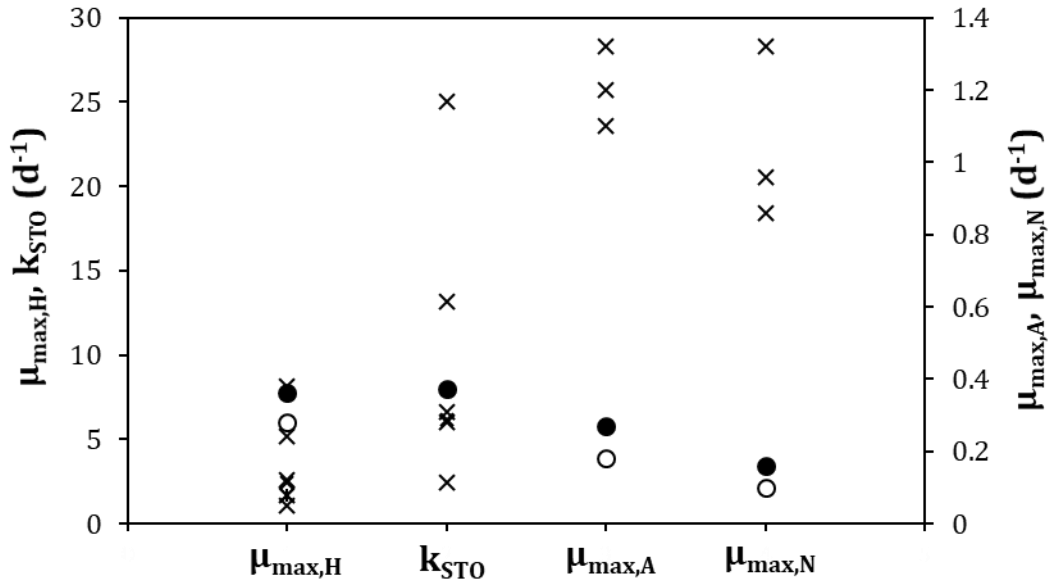


220

221 Figure 2: Results of the ASM3 model calibration (a,b) and validation (c,d). Cyclic concentration profiles  
 222 in the AGS for (a,c)  $S_{\text{COD}}$  and  $S_{\text{S}}$  and for (b,d)  $S_{\text{NH}}$  and  $S_{\text{NO}_2}$ . Markers represent experimental data; full  
 223 lines denote simulation results.

224 Heterotrophic bacteria ( $X_{\text{H}}$ ) were present in the external layers of the granule, whereas  
 225 autotrophs ( $X_{\text{A}}$ ) were located in inner layers of the granule, due to the lower growth rates  
 226 compared to heterotrophs (Figure S.3). There was a progressive increase of the inert material  
 227 ( $X_{\text{I}}$ ) in direction to the centre of the granule, which indicates an important fraction of the  
 228 granule which is not active.

229 The calibrated heterotrophic bacteria kinetic parameters ( $\mu_{\text{max,H}}$  of  $6 \text{ d}^{-1}$  and  $k_{\text{STO}}$  of  $8 \text{ d}^{-1}$ ) were  
 230 similar to those from previous research works modelling AGS with ASM3 (Figure 3).



231

232 Figure 3: Comparison of the kinetic parameters of this model (with (●) and without (○) adding the salt  
 233 inhibition term) with the values obtained in other studies (x) modelling AGS with ASM3 [16,20–24].

234 However, the calibrated values of nitrifying bacteria ( $\mu_{max,A}$  of 0.18 and  $\mu_{max,N}$  of 0.10 d<sup>-1</sup>)  
 235 were lower than the reported ranges of 1.1 – 1.3 and 0.9 – 1.3 d<sup>-1</sup> for  $\mu_{max,A}$  and  $\mu_{max,N}$ ,  
 236 respectively [20–24].

237 These low values could be attributed to a number of reasons. First, one of the possible causes  
 238 for low values of  $\mu_{max,A}$  and  $\mu_{max,N}$  may be a high biomass retention inside the reactor (in this  
 239 study the Sludge Retention Time (SRT) was 10 – 15 d). Chiellini et al [31] estimated the value  
 240 of  $\mu_{max,A}$  in a Conventional Activated Sludge (CAS) reactor and a Membrane bioreactor  
 241 (MBR). They observed a lower value of 0.46 d<sup>-1</sup> in MBR, with a SRT of 20 days, whereas in  
 242 CAS it was of 0.96 d<sup>-1</sup> (SRT below 10 d). Munz et al. [32] also established a comparison  
 243 between CAS and MBR and observed the same results, a  $\mu_{max,A}$  of 0.35 d<sup>-1</sup> in an MBR and of  
 244 0.72 d<sup>-1</sup> in CAS. They pointed out that the cause could be the difference between the SRT of  
 245 both systems (20 d in the MBR, 8 d in the CAS). In systems with biofilms the higher biomass  
 246 retention and SRT promote the selection of slow-growing nitrifiers, which present low values  
 247 of  $\mu_{max}$ . The SRT values of the AGS reactor in this study are more comparable to MBR systems,

248 for this reason the development of slow-growing nitrifiers (low values of  $\mu_{\max}$ ) is favoured [31,  
249 32].

250 Another factor that could reduce the value of  $\mu_{\max,A}$  is the salt concentration inside the reactor  
251 (in this study the salt concentration fluctuated between 5 – 13 g NaCl/L). Cui et al. [33]  
252 observed that the increase of the salt concentration (30 – 85 g NaCl/L) stimulates the growth  
253 of halophilic nitrifiers, characterised by a high affinity for ammonium and low growth rates  
254 (low half-saturation constant and low  $\mu_{\max}$ ). They determined a  $\mu_{\max}$  of 0.26 d<sup>-1</sup> with a salt  
255 concentration of 30 g NaCl/L and half-saturation coefficient values of 1 – 1.7 mg NH<sub>4</sub><sup>+</sup>-N/L.  
256 The kinetic parameters showed a decreasing trend with the increase of salinity. They suggested  
257 the possibility of a shift in the community composition due to a long-term salinity selection.  
258 Gonzalez-Silva et al. [34] also observed a change with time of the microbial community  
259 composition as a response to the variations on salt concentration and its adaptation to saline  
260 conditions. Although the salt concentration tested in the current study (5 – 13 g NaCl/L) was  
261 lower than in the abovementioned previous works (30 – 85 g NaCl/L), the inoculum of the  
262 reactor came from a biological reactor of a fish cannery, adapted to even higher salinity, so the  
263 nitrifying bacteria might be different populations compared to an inoculum non-adapted to  
264 salinity.

265 Additionally, a few studies have also reported values of  $\mu_{\max,A}$  lower than those in ASM3. Gao  
266 et al. [35] obtained a value of 0.46 d<sup>-1</sup>. They explained that it was due to the shortcut  
267 nitrification process, with only nitrite production. The biomass production, in this case, was  
268 less than in the conventional nitrification process considered in ASM3 (AOB+NOB activity in  
269 a single process). Consequently, the value of  $\mu_{\max}$  was lower than ASM3.

270 In this study, the calibrated values ( $\mu_{\max,A}$  of 0.18 and  $\mu_{\max,N}$  of 0.10 d<sup>-1</sup>) obtained in this study  
271 are still somewhat lower than those from literature (0.46 [31,35], 0.35 [32], 0.26 [33] d<sup>-1</sup>). This

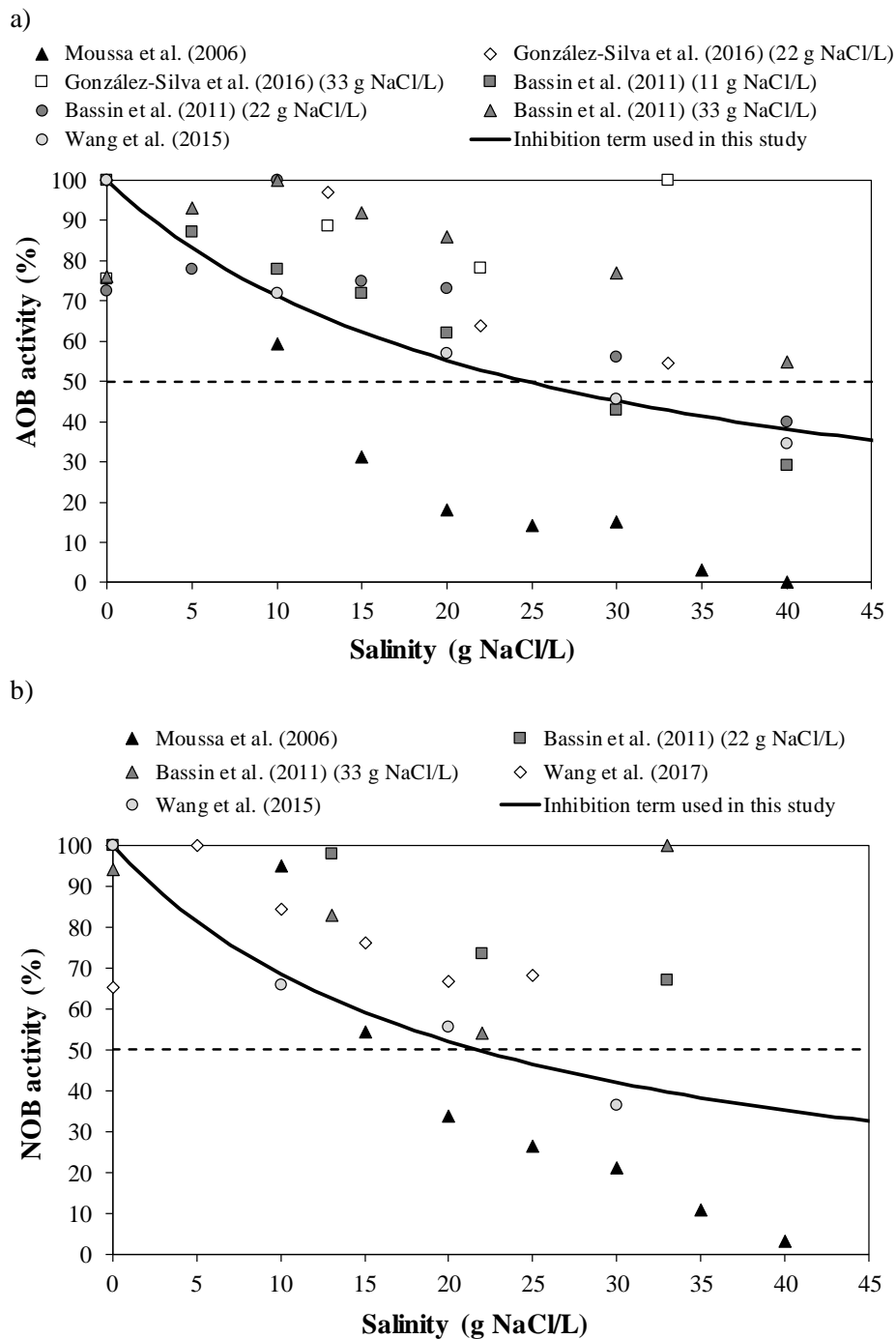
272 could be due to the combination of the three causes mentioned before (SRT of 15 days, salinity  
273 of 13 g/L and only nitrification).

#### 274 **4.3. Addition of salinity effects**

275 Since salinity was likely one of the causes for the low values of the maximum growth rates, the  
276 salinity inhibition term was added to the model to explicitly consider its effects on the different  
277 bacterial populations. This allowed the comparison between the maximum growth rates of this  
278 study with other research works regardless of the salt concentration (Figure 3).

279 To estimate the salinity inhibition constant of each bacterial population, firstly a literature  
280 review was made about the reported decrease of the biological activity of biofilms (mainly  
281 AGS) with the increase of salinity. The gathered data was divided into two groups: biological  
282 activity reduction of (1) biomass adapted and (2) non-adapted to salinity. In this study, data  
283 from group (1) (Figure 4) was used to estimate the inhibition constant, since the cultivated AGS  
284 was adapted to the presence of salt. Additionally, data corresponding to non-adapted biomass  
285 (not used in this study) can be found in supplementary materials (Figure S.1). The activity  
286 reduction of the different types of bacteria from different studies was plotted. Then, the half-  
287 saturation constant was estimated by reading in the figures the salt concentration corresponding  
288 to the 50 % decrease of the maximum activity (dashed line).

289 The inhibition constant of heterotrophic bacteria was determined based on values reported in  
290 literature [36] due to the lack of specific activity assays at different salt concentrations. This  
291 study reports the reduction of the biological activity of AGS with the gradual increase of  
292 salinity in a sequencing batch reactor.



293

294 Figure 4: (a) AOB activity and (b) NOB activity with different salt concentrations of biomass adapted  
 295 to salinity.

296 With the addition of the salinity term to the model, the maximum growth rates were re-  
 297 calculated to provide the same results as Figure 2 (a,b). The calibrated values were higher than  
 298 in the previous section: 0.27, 0.16 and 7.76 d<sup>-1</sup> for AOB, NOB and heterotrophs, respectively  
 299 (Figure 3), while the conversion rates were the same. This indicates that the addition of the

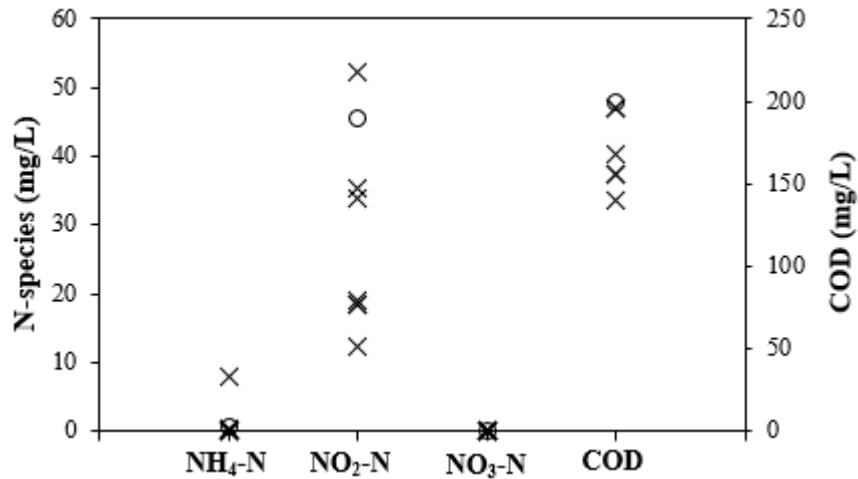
300 inhibition term could reproduce the experimental findings. Regarding the biological activity  
301 inhibition, heterotrophic bacteria were the least affected by the presence of salt. The COD  
302 conversion rate was reduced 23 and 10 % under salinity conditions corresponding to calibration  
303 and validation, respectively. AOB and NOB activities suffered higher reductions, especially  
304 with the salt concentration of 13 g NaCl/L (calibration, 34 and 37% activity reduction for AOB  
305 and NOB, respectively), showing a higher sensitivity of nitrifying bacteria to the increase of  
306 salinity.

#### 307 **4.4. Model validation**

308 In the validation step, the results of the model (the salinity inhibition term was included) were  
309 compared with an operational cycle at a salinity of 5 g NaCl/L. The COD consumption was  
310 accurately reproduced (Figure 2,c). However, the predicted ammonia oxidation was faster than  
311 the experimental data (Figure 2,d). The ammonia and nitrite concentration of the effluent were  
312 underestimated and overestimated respectively, both in a 65 % (calculated as the difference  
313 between the experimental and the model value, divided by the experimental value). This could  
314 be due to the fact that the experimental cycle measurement was done in a moment when the  
315 reactor was not working in steady-state conditions. A few days before the cycle measurement  
316 (days 196 – 209), the washout of part of the biomass took place, associated to the change of  
317 salinity [7]. Although a stable effluent quality was achieved in these days, the biomass might  
318 have been still adapting to the new conditions of the reactor.

319 In order to validate the model with experimental data from steady-state conditions, the effluent  
320 quality predicted by the model was also compared with the effluent quality measured  
321 experimentally during phase IV before the washout of the biomass (Figure 5). The results  
322 indicate that, despite the different conversion rates of AOB, the model was able to predict the  
323 effluent concentrations of both organic matter and nitrogen compounds.





324

325 Figure 5: Comparison of the effluent quality from the experimental data of phase IV (x) and  
 326 predicted by the model (o).

327 The biokinetic model considering the inhibition of salinity on the biological activity was  
 328 calibrated with a representative cycle measurement from an operational phase of an AGS  
 329 reactor with 13 g NaCl/L. In addition, it was validated with the effluent measurements of a  
 330 different phase, with 5 g NaCl/L. However, the model has some shortcomings. It was observed  
 331 experimentally that salt fluctuations not only affected the biological activity, but also the  
 332 physical properties of the biomass [7]. In this model, only the effect of salinity on the  
 333 bioconversion processes was considered. In addition, the salt concentrations used as input of  
 334 the model were low-moderate, and the model should be tested with higher concentrations (20  
 335 – 40 g NaCl/L). Further research is needed to (1) test the biological model with a wider range  
 336 of salt concentrations to assess the impact of salinity on the biological activity and (2) study  
 337 the feasibility of incorporating also the effect of salinity on the physical properties of the  
 338 biomass. Additionally, further research is needed to clarify what is exactly the effect of salinity  
 339 on the bacterial populations: inhibition, shift of bacterial populations or a combination of both.  
 340 This will further help to determine if an inhibition term is sufficient for a proper description of  
 341 reactor performance or if it is more important to re-calibrate the growth rates according to the  
 342 specific bacterial communities present in the reactor. This model could be further used as a

343 starting point for future research. For instance, the model could be applied in the design stage  
344 of future AGS reactors or for system optimization and scenario analysis of existing reactors  
345 treating saline wastewater.

## 346 **5. CONCLUSIONS**

347 In this study, an ASM3-based biofilm model was demonstrated suitable to describe the  
348 performance (COD and N conversions) of an AGS reactor with a short feeding phase treating  
349 industrial saline wastewater. ASM1 could not predict the COD conversion rates observed  
350 experimentally, which underlined the importance of explicitly describing substrate storage.

351 Model calibration revealed unusually low growth rates for nitrifying bacteria, which was  
352 mainly attributed to the effect of salinity, combined with other factors such as a high SRT. The  
353 presence of salt also provoked nitrite accumulation. The addition of a non-competitive  
354 inhibitory term to the model could accurately predict the COD and nitrogen conversions in the  
355 AGS reactor under different salinities.

## 356 **6. ACKNOWLEDGEMENTS**

357 We thank Janis Baeten for the interesting discussions on this topic. P. Carrera acknowledges  
358 CRETUS Strategic Partnership (ED431E 2018/01) for financial support. The authors from the  
359 USC belong to the Galician Competitive Research Group (GRC ED431C 2017/29) and the  
360 CRETUS Strategic Partnership (ED431E 2018/01). All these programs are co-financed by  
361 FEDER (EU) funds. The doctoral research work of L. Strubbe has been financially supported  
362 by a Doctoral fellowship of the Research Foundation – Flanders (FWO PhD fellowship  
363 strategic basic research 1SC1220N).

364

## 365 7. REFERENCES

- 366 [1] M. Pronk, M.K. de Kreuk, B. de Bruin, P. Kamminga, R. Kleerebezem, M.C.M. van Loosdrecht,  
367 Full scale performance of the aerobic granular sludge process for sewage treatment, *Water Res.*  
368 84 (2015) 207–217. <https://doi.org/10.1016/j.watres.2015.07.011>.
- 369 [2] B. van den Akker, K. Reid, K. Middlemiss, J. Krampe, Evaluation of granular sludge for  
370 secondary treatment of saline municipal sewage, *J. Environ. Manage.* 157 (2015) 139–145.  
371 <https://doi.org/10.1016/j.jenvman.2015.04.027>.
- 372 [3] B.J. Thwaites, B. Van Den Akker, P.J. Reeve, M.D. Short, N. Dinesh, J.P. Alvarez-Gaitan, R.  
373 Stuetz, Ecology and performance of aerobic granular sludge treating high-saline municipal  
374 wastewater, *Water Sci. Technol.* (2018). <https://doi.org/10.2166/wst.2017.626>.
- 375 [4] R. Campo, G. Di Bella, Petrochemical slop wastewater treatment by means of aerobic granular  
376 sludge: effect of granulation process on bio-adsorption and hydrocarbons removal, *Chem. Eng.*  
377 *J.* (2019). <https://doi.org/10.1016/j.cej.2019.122083>.
- 378 [5] S.F. Corsino, M. Capodici, C. Morici, M. Torregrossa, G. Viviani, Simultaneous nitrification-  
379 denitrification for the treatment of high-strength nitrogen in hypersaline wastewater by aerobic  
380 granular sludge, *Water Res.* 88 (2016) 329–336. <https://doi.org/10.1016/j.watres.2015.10.041>.
- 381 [6] A. Val del Río, M. Figueroa, B. Arrojo, A. Mosquera-Corral, J.L. Campos, G. García-Torriello,  
382 R. Méndez, Aerobic granular SBR systems applied to the treatment of industrial effluents, *J.*  
383 *Environ. Manage.* (2012). <https://doi.org/10.1016/j.jenvman.2011.03.019>.
- 384 [7] P. Carrera, R. Campo, R. Méndez, G. Di Bella, J.L. Campos, A. Mosquera-Corral, A. Val del  
385 Rio, Does the feeding strategy enhance the aerobic granular sludge stability treating saline  
386 effluents?, *Chemosphere.* (2019). <https://doi.org/10.1016/j.chemosphere.2019.03.127>.
- 387 [8] J.P. Bassin, M. Pronk, G. Muyzer, R. Kleerebezem, M. Dezotti, M.C.M. van Loosdrecht, Effect  
388 of elevated salt concentrations on the aerobic granular sludge process: Linking microbial activity  
389 with microbial community structure, *Appl. Environ. Microbiol.* (2011).  
390 <https://doi.org/10.1128/AEM.05016-11>.
- 391 [9] S.F. Corsino, M. Capodici, C. Morici, M. Torregrossa, G. Viviani, Simultaneous nitrification-  
392 denitrification for the treatment of high-strength nitrogen in hypersaline wastewater by aerobic  
393 granular sludge, *Water Res.* (2016). <https://doi.org/10.1016/j.watres.2015.10.041>.
- 394 [10] X. Li, J. Luo, G. Guo, H.R. Mackey, T. Hao, G. Chen, Seawater-based wastewater accelerates  
395 development of aerobic granular sludge: A laboratory proof-of-concept, *Water Res.* (2017).  
396 <https://doi.org/10.1016/j.watres.2017.03.002>.

- 397 [11] X. Wang, T. Yang, B. Lin, Y. Tang, Effects of salinity on the performance, microbial  
398 community, and functional proteins in an aerobic granular sludge system, *Chemosphere*. (2017).  
399 <https://doi.org/10.1016/j.chemosphere.2017.06.047>.
- 400 [12] M. Pronk, J.P. Bassin, M.K. De Kreuk, R. Kleerebezem, M.C.M. Van Loosdrecht, Evaluating  
401 the main and side effects of high salinity on aerobic granular sludge, *Appl. Microbiol.*  
402 *Biotechnol.* (2014). <https://doi.org/10.1007/s00253-013-4912-z>.
- 403 [13] M. Figueroa, A. Mosquera-Corral, J.L. Campos, R. Méndez, Treatment of saline wastewater in  
404 SBR aerobic granular reactors, *Water Sci. Technol.* (2008).  
405 <https://doi.org/10.2166/wst.2008.406>.
- 406 [14] M.S. Moussa, D.U. Sumanasekera, S.H. Ibrahim, H.J. Lubberding, C.M. Hooijmans, H.J.  
407 Gijzen, M.C.M. Van Loosdrecht, Long term effects of salt on activity, population structure and  
408 floc characteristics in enriched bacterial cultures of nitrifiers, *Water Res.* (2006).  
409 <https://doi.org/10.1016/j.watres.2006.01.029>.
- 410 [15] J.E. Baeten, D.J. Batstone, O.J. Schraa, M.C.M. van Loosdrecht, E.I.P. Volcke, Modelling  
411 anaerobic, aerobic and partial nitrification-anammox granular sludge reactors - A review, *Water*  
412 *Res.* 149 (2019) 322–341. <https://doi.org/10.1016/j.watres.2018.11.026>.
- 413 [16] M. Henze, W. Gujer, T. Mino, M. van Loosdrecht, Activated Sludge Models ASM1, ASM2,  
414 ASM2d and ASM3 IWA Scientific and Technical Report No.9, 2000.  
415 <https://doi.org/10.1017/CBO9781107415324.004>.
- 416 [17] M. Henze, W. Gujer, T. Mino, M. van Loosdrecht, Activated Sludge Models ASM1, ASM2,  
417 ASM2d and ASM3 IWA Scientific and Technical Report No.9, 2000.  
418 <https://doi.org/10.1017/CBO9781107415324.004>.
- 419 [18] G. Sin, P.A. Vanrolleghem, Evolution of an ASM2d-like model structure due to operational  
420 changes of an SBR process, *Water Sci. Technol.* 53 (2006) 237–245.  
421 <https://doi.org/10.2166/wst.2006.426>.
- 422 [19] D. Kaelin, R. Manser, L. Rieger, J. Eugster, K. Rottermann, H. Siegrist, Extension of ASM3 for  
423 two-step nitrification and denitrification and its calibration and validation with batch tests and  
424 pilot scale data, *Water Res.* (2009). <https://doi.org/10.1016/j.watres.2008.12.039>.
- 425 [20] B.J. Ni, H.Q. Yu, Y.J. Sun, Modeling simultaneous autotrophic and heterotrophic growth in  
426 aerobic granules, *Water Res.* (2008). <https://doi.org/10.1016/j.watres.2007.11.010>.
- 427 [21] M. Zhou, J. Gong, C. Yang, W. Pu, Simulation of the performance of aerobic granular sludge  
428 SBR using modified ASM3 model, *Bioresour. Technol.* (2013).

- 429 <https://doi.org/10.1016/j.biortech.2012.09.076>.
- 430 [22] J.R. Vázquez-Padín, A. Mosquera-Corral, J.L. Campos, R. Méndez, J. Carrera, J. Pérez,  
431 Modelling aerobic granular SBR at variable COD/N ratios including accurate description of total  
432 solids concentration, *Biochem. Eng. J.* (2010). <https://doi.org/10.1016/j.bej.2009.12.009>.
- 433 [23] E. Isanta, M. Figueroa, A. Mosquera-Corral, L. Campos, J. Carrera, J. Pérez, A novel control  
434 strategy for enhancing biological N-removal in a granular sequencing batch reactor: A model-  
435 based study, *Chem. Eng. J.* (2013). <https://doi.org/10.1016/j.cej.2013.07.118>.
- 436 [24] J. Zhao, J. Huang, M. Guan, Y. Zhao, G. Chen, X. Tian, Mathematical simulating the process of  
437 aerobic granular sludge treating high carbon and nitrogen concentration wastewater, *Chem. Eng.*  
438 *J.* (2016). <https://doi.org/10.1016/j.cej.2016.07.098>.
- 439 [25] C. Krishna, M.C.M. Van Loosdrecht, Substrate flux into storage and growth in relation to  
440 activated sludge modeling, *Water Res.* (1999). [https://doi.org/10.1016/S0043-1354\(99\)00031-](https://doi.org/10.1016/S0043-1354(99)00031-7)  
441 [7](https://doi.org/10.1016/S0043-1354(99)00031-7).
- 442 [26] J.E. Baeten, M.C.M. van Loosdrecht, E.I.P. Volcke, Improving the accuracy of granular sludge  
443 and biofilm reactor simulations in Aquasim through artificial diffusion, *Biotechnol. Bioeng.*  
444 (2017). <https://doi.org/10.1002/bit.26323>.
- 445 [27] J.E. Baeten, M.C.M. van Loosdrecht, E.I.P. Volcke, Modelling aerobic granular sludge reactors  
446 through apparent half-saturation coefficients, *Water Res.* (2018).  
447 <https://doi.org/10.1016/j.watres.2018.09.025>.
- 448 [28] P. Reichert, Aquasim - A tool for simulation and data analysis of aquatic systems, in: *Water Sci.*  
449 *Technol.*, 1994.
- 450 [29] B.E. Rittmann, J.P. Boltz, D. Brockmann, G.T. Daigger, E. Morgenroth, K.H. Sørensen, I.  
451 Takács, M. Van Loosdrecht, P.A. Vanrolleghem, A framework for good biofilm reactor  
452 modeling practice (GBRMP), *Water Sci. Technol.* 77 (2018) 1149–1164.  
453 <https://doi.org/10.2166/wst.2018.021>.
- 454 [30] M. Zhou, J. Gong, C. Yang, W. Pu, Simulation of the performance of aerobic granular sludge  
455 SBR using modified ASM3 model, *Bioresour. Technol.* 127 (2013) 473–481.  
456 <https://doi.org/10.1016/j.biortech.2012.09.076>.
- 457 [31] C. Chiellini, G. Munz, G. Petroni, C. Lubello, G. Mori, F. Verni, C. Vannini, Characterization  
458 and comparison of bacterial communities selected in conventional activated sludge and  
459 membrane bioreactor pilot plants: A focus on nitrospira and planctomycetes bacterial phyla,  
460 *Curr. Microbiol.* (2013). <https://doi.org/10.1007/s00284-013-0333-6>.

- 461 [32] G. Munz, G. Mori, C. Vannini, C. Lubello, Kinetic parameters and inhibition response of  
462 ammonia-and nitrite-oxidizing bacteria in membrane bioreactors and conventional activated  
463 sludge processes, *Environ. Technol.* (2010). <https://doi.org/10.1080/09593331003793828>.
- 464 [33] Y.W. Cui, H.Y. Zhang, J.R. Ding, Y.Z. Peng, The effects of salinity on nitrification using  
465 halophilic nitrifiers in a Sequencing Batch Reactor treating hypersaline wastewater, *Sci. Rep.*  
466 (2016). <https://doi.org/10.1038/srep24825>.
- 467 [34] B.M. Gonzalez-Silva, K.R. Jonassen, I. Bakke, K. Østgaard, O. Vadstein, Nitrification at  
468 different salinities: Biofilm community composition and physiological plasticity, *Water Res.* 95  
469 (2016) 48–58. <https://doi.org/10.1016/j.watres.2016.02.050>.
- 470 [35] D. Gao, Y. Peng, W.M. Wu, Kinetic model for biological nitrogen removal using shortcut  
471 nitrification-denitrification process in sequencing batch reactor, *Environ. Sci. Technol.* (2010).  
472 <https://doi.org/10.1021/es100514x>.
- 473 [36] Z. Wang, M. Gao, Z. She, S. Wang, C. Jin, Y. Zhao, S. Yang, L. Guo, Effects of salinity on  
474 performance, extracellular polymeric substances and microbial community of an aerobic  
475 granular sequencing batch reactor, *Sep. Purif. Technol.* (2015).  
476 <https://doi.org/10.1016/j.seppur.2015.02.042>.